

Liyuan Weng^{1*}, Ping Liang², Yanluan Lin¹¹Department of Earth System Science, Tsinghua University, Beijing, China²Shanghai Regional Climate Center, China Meteorological Administration, Shanghai, China

1. INTRODUCTION

In boreal summer, precipitation in eastern China shows remarkable intraseasonal variation, most of which comes from the tropics (Ren et al. 2022) and can be accounted by the boreal summer intraseasonal oscillation (BSISO) (Lee et al. 2013; Zhang et al. 2009). The BSISO, the counterpart of the MJO in boreal summer, is an intraseasonal (30-60-day), planetary-scale, and slowly northeastward-propagating convective envelope, primarily active in the Indian Ocean and the northwestern Pacific (Kikuchi 2021) and can be influenced by the background sea surface temperature (SST) in both tropics and extratropics (Wang and Xie 1997; Zhou et al. 2024; Lee et al. 2022).

Because the BSISO provides one of the most important predictability sources for subseasonal to seasonal precipitation forecasts (Li 2023; Meehl et al. 2021), the effect of the BSISO on the eastern China precipitation has received much attention. As the BSISO moves from the Indian Ocean to the northwestern Pacific, the vertical motion anomaly in eastern China transforms from ascending to descending and the moisture transport decreases (Ju et al. 2023; Li and Mao 2018; Qi et al. 2019). As a result, the precipitation in eastern China is firstly enhanced and then suppressed (Zhang et al. 2009). This effect has been observed in both southern part and northern part of eastern China (Gao et al. 2022; Hao et al. 2023; Li and Lu 2018). However, whether the location of the BSISO-related precipitation varies remains elusive. Characteristics of total precipitation, such as the location, orientation, extent, and amount, have been shown to be associated with the large-scale circulation, including northwestern Pacific subtropical high and the mid-latitude westerly jet (Du et al. 2020, 2022; Qi et al. 2019; Sampe and Xie 2010), and it is desirable to find some potential predictors (Pan and Lu 2022; Yu and Zhai 2022).

This study will focus on the intraseasonal part of the total precipitation, which can facilitate summer precipitation forecasts.

2. DATA AND METHODS

We use the Climate Prediction Center (CPC) Unified Gauge-Based Analysis of Global Daily Precipitation and the Environmental Prediction-National Center for Atmospheric Research (NCEP/NCAR) Reanalysis to investigate the eastern China (105°-122.5°E, 20°-40°N) precipitation in boreal summer (May, June, July, and August) during 1981-2022. The monthly SST are obtained from the National Oceanic and Atmospheric Administration (NOAA) Extended Reconstructed SST analysis, version 5 (ERSSTv5). We also use the daily NOAA outgoing longwave radiation (OLR) to describe the BSISO-related convection. For the daily precipitation, OLR, and atmospheric variables from the reanalysis, the annual cycle and the long-term linear mean are removed and then a 30-60-day bandpass Lanczos filter is used to extract BSISO-related variability,

To identify the BSISO activity, we adopt the daily BSISO1 index (Lee et al. 2013). The amplitude of the index is defined as the root sum of squares of the two corresponding principal components and indicates the strength of the BSISO. The two components of the index divide the active BSISO into eight phases, representing the location of the BSISO. In the phases 2, 3, and 4, convection is active over the Indian Ocean and the precipitation in eastern China is enhanced. These three phases are hereinafter called the wet spell.

Since the precipitation area in eastern China in summer mostly appears as a zonally-elongated rainband, the location of the BSISO-related precipitation can be represented as the latitudinal centroid of the area with positive precipitation anomaly during the wet spell in each year, weighted

* *Corresponding author address*: Liyuan Weng, Department of Earth System Science, Tsinghua University, Beijing, 100084, China; email: wengly20@mails.tsinghua.edu.cn

by the precipitation anomaly and the cosine of the latitude (Zhou et al. 2020).

3. RESULTS

The composite precipitation clearly shows the BSISO-related precipitation in eastern China. During the phases 2, 3, and 4, the BSISO-related precipitation is significant in a wide area, between 25°N and 35°N (Figure 1a) with the latitudinal centroid around 29°N (blue dashed lines in Figure 1a and 1b). The BSISO-related precipitation concentrating around 29°N after long-term averaging (the blue dashed line in Figure 1a and 1b), but the latitudinal centroid of the BSISO-related precipitation shows great interannual variability around the long-term mean (Figure 1b). The amplitude of the variability is around 8 degrees or 900km, from the southern China (25.5°N) to the Huai River basin (33.4°N). We then composite years with latitude one standard deviation away from the mean. The “south years” (1981, 1986, 1995, 2001, 2005, and 2019) is defined as the precipitation location one standard deviation below the mean and the “north years” (1982, 1991, 2000, 2006, 2007, 2012, 2013, 2016, and 2020) as one standard deviation above the mean latitude (Figure 1b).

The composite precipitation anomalies clearly show the location difference (Figure 2a). The positive anomalies locate in the southern edge of the mid-latitude easterly jet at 200 hPa. As the westerly jet moves northward, the ascending motion also moves from 25°N to 35°N (Figure 2e and 2f). At 850 hPa, the anomalous anticyclone in the subtropical northwestern Pacific extends westward in the north years and the associated southwesterly wind in the northwestern flank of the anticyclone also moves northwestward (Figures 2c and 2d). The mid-latitude westerly jet at 200 hPa and the subtropical anomalous anticyclone provides favorable dynamical conditions synergistically.

Apart from the dynamical conditions, moisture conditions are also important for precipitation in eastern China. The BSISO convection heating over the Indian Ocean triggers a Gill-like pattern (Gill, 1980), that is, in the lower troposphere, two cyclones straddling the equator to the west and enhanced easterly wind to the east (Figures 2c and 2d). The low-level circulation transports moisture and leads to moisture convergence in the eastern edge of the BSISO convection area as well as along the northwestern flank of the northwestern Pacific subtropical high (Figures 3a and 3b). In the north

years, the northwestern Pacific subtropical high extends westward and the BSISO convection also moves northward in the Indian Ocean. As a result, the moisture convergence in eastern China also moves northward, favoring the northward moving of the BSISO-related precipitation.

The correlation map between the SST anomalies and the latitude of BSISO-related precipitation shows that only extratropical Pacific show persistent correlation from February to May (Figures 4a-d). In February, in the northeastern Pacific along the North America coast, SST has a negative correlation with the latitude of the BSISO-related precipitation. The negative correlation area extends southwestward to the central tropical Pacific. The correlation starts to develop in the preceding winter and peaks in March (a two-month lead) with value -0.40 (black line in Figure 4e). At the same time, the central northern Pacific shows positive correlation and also becomes statistically significant in March and May. Both correlations decay after May.

Warm SST anomalies in the central Northern Pacific favors northward shifting of the mid-latitude westerly jet by heating the troposphere locally and thus decreasing the meridional temperature gradient south of this area. On the other hand, the cold SST anomalies in the northeastern Pacific favors a northeast-southwest-tilting westerly jet, which also indicates a northward shifting of the jet in eastern China (Du et al., 2016).

4. CONCLUSIONS AND DISCUSSIONS

In this study, we show that the location of BSISO-related precipitation in eastern China displays clear interannual variations, which is determined by the location of both the mid-latitude westerly jet and the northwestern Pacific subtropical high. The precipitation location is also significantly correlated with extratropical Pacific SST because warm central northern Pacific and cold northeastern Pacific favor a northward shifting of mid-latitude westerly jet. Combined with the westward extend of the subtropical high, both moisture transport and ascending motion move northward. And the precipitation anomaly northward moves accordingly over eastern China.

The extratropical Pacific SST anomaly pattern is similar to the Northern Pacific Meridional Mode (PMM) (Chiang & Vimont, 2004) and the high correlation area in the southern Pacific (Figure 4a-d) also suggests the possible role of the meridional mode (H. Zhang et al., 2014). A negative PMM can also

strengthen the northwestern Pacific subtropical high (W. Zhang et al., 2016) and thus moves the BSISO-related precipitation northward. In fact, the correlation of the PMM index in March and the location is significant at a significance level of 0.05, with value of -0.3. This provides a potential predictor for the location of the precipitation with about two months lead and facilitates subseasonal to seasonal forecast in eastern China precipitation.

REFERENCES

- Du, Y., Z. Xie, and Q. Miao, 2020: Spatial Scales of Heavy Meiyu Precipitation Events in Eastern China and Associated Atmospheric Processes. *Geophys. Res. Lett.*, **47**, e2020GL087086, <https://doi.org/10.1029/2020GL087086>.
- , —, N. Wang, Q. Miao, and L. Zhang, 2022: Influence of Zonal Variation of the Subtropical Westerly Jet on Rainfall Patterns and Frequency of Heavy Precipitation Events over East Asia. *Journal of Climate*, **35**, 6611–6626, <https://doi.org/10.1175/JCLI-D-21-0872.1>.
- Gao, Y., P.-C. Hsu, S. Che, C. Yu, and S. Han, 2022: Origins of Intraseasonal Precipitation Variability over North China in the Rainy Season. *Journal of Climate*, **35**, 6219–6236, <https://doi.org/10.1175/JCLI-D-21-0832.1>.
- Hao, L., T. Li, L. Zhang, and N. Ma, 2023: Influence of boreal summer intraseasonal oscillation on summer precipitation in North China. *International Journal of Climatology*, **43**, 4816–4834, <https://doi.org/10.1002/joc.8118>.
- Ju, Z., J. Rao, Y. Wang, J. Yang, and Q. Lu, 2023: Modulation of the intraseasonal variability in early summer precipitation in eastern China by the Quasi-Biennial Oscillation and the Madden–Julian Oscillation. *Atmospheric Chemistry and Physics*, **23**, 14903–14918, <https://doi.org/10.5194/acp-23-14903-2023>.
- Kikuchi, K., 2021: The Boreal Summer Intraseasonal Oscillation (BSISO): A Review. *Journal of the Meteorological Society of Japan. Ser. II*, **99**, 933–972, <https://doi.org/10.2151/jmsj.2021-045>.
- Lee, D. Y., J.-Y. Lee, Y.-M. Yang, P.-C. Hsu, and J.-E. Kim, 2022: Dominant Processes for Dependence of Boreal Summer Intraseasonal Oscillation on El Niño Phases. *Geophys. Res. Lett.*, **49**, e2022GL098669, <https://doi.org/10.1029/2022GL098669>.
- Lee, J.-Y., B. Wang, M. C. Wheeler, X. Fu, D. E. Waliser, and I.-S. Kang, 2013: Real-time multivariate indices for the boreal summer intraseasonal oscillation over the Asian summer monsoon region. *Clim. Dyn.*, **40**, 493–509, <https://doi.org/10.1007/s00382-012-1544-4>.
- Li, J., and J. Mao, 2018: The impact of interactions between tropical and midlatitude intraseasonal oscillations around the Tibetan Plateau on the 1998 Yangtze floods. *Quarterly Journal of the Royal Meteorological Society*, **144**, 1123–1139, <https://doi.org/10.1002/qj.3279>.
- Li, X., 2023: Subseasonal Predictability of Early and Late Summer Rainfall over East Asia. *Journal of Climate*, **36**, 8513–8523, <https://doi.org/10.1175/JCLI-D-23-0183.1>.
- Li, X., and R. Lu, 2018: Subseasonal Change in the Seesaw Pattern of Precipitation between the Yangtze River Basin and the Tropical Western North Pacific during Summer. *Adv. Atmos. Sci.*, **35**, 1231–1242, <https://doi.org/10.1007/s00376-018-7304-6>.
- Meehl, G. A., and Coauthors, 2021: Initialized Earth System Prediction from Subseasonal to Decadal Timescales. *Nat. Rev. Earth Environ.*, **2**, 340–357, <https://doi.org/10.1038/s43017-021-00155-x>.
- Pan, M., and M. Lu, 2022: Long-Lead Predictability of Western North Pacific Subtropical High. *Journal of Geophysical Research: Atmospheres*, **127**, e2021JD035967, <https://doi.org/10.1029/2021JD035967>.
- Qi, Y., T. Li, R. Zhang, and Y. Chen, 2019: Interannual relationship between intensity of rainfall intraseasonal oscillation and summer-mean rainfall over Yangtze River Basin in eastern China. *Clim Dyn*, **53**, 3089–3108, <https://doi.org/10.1007/s00382-019-04680-w>.
- Ren, Q., F. Liu, B. Wang, S. Yang, H. Wang, and W. Dong, 2022: Origins of the Intraseasonal Variability of East Asian Summer Precipitation. *Geophys. Res. Lett.*, **49**, e2021GL096574, <https://doi.org/10.1029/2021GL096574>.
- Sampe, T., and S.-P. Xie, 2010: Large-Scale Dynamics of the Meiyu-Baiu Rainband: Environmental Forcing by the Westerly Jet. *Journal of Climate*, **23**, 113–134, <https://doi.org/10.1175/2009JCLI3128.1>.
- Wang, B., and X. Xie, 1997: A model for the boreal

- summer intraseasonal oscillation. *J. Atmos. Sci.*, **54**, 72–86, [https://doi.org/10.1175/1520-0469\(1997\)054<0072:AMFTBS>2.0.CO;2](https://doi.org/10.1175/1520-0469(1997)054<0072:AMFTBS>2.0.CO;2).
- Yu, R., and P. Zhai, 2022: An objective approach to predict the spatial property of anomalous rain-belt of Meiyu. *Weather Clim. Extremes*, **37**, 100466, <https://doi.org/10.1016/j.wace.2022.100466>.
- Zhang, L., B. Wang, and Q. Zeng, 2009: Impact of the Madden–Julian Oscillation on Summer Rainfall in Southeast China. *J. Clim.*, **22**, 201–216, <https://doi.org/10.1175/2008JCLI1959.1>.
- Zhou, H., P.-C. Hsu, L. Chen, and Y. Qian, 2024: Interannual variability of boreal summer intraseasonal oscillation over the northwestern Pacific influenced by the Pacific Meridional Mode. *Atmospheric and Oceanic Science Letters*, 100492, <https://doi.org/10.1016/j.aosl.2024.100492>.
- Zhou, W., D. Yang, S.-P. Xie, and J. Ma, 2020: Amplified Madden–Julian oscillation impacts in the Pacific–North America region. *Nat. Clim. Change*, **10**, 654–660, <https://doi.org/10.1038/s41558-020-0814-0>.

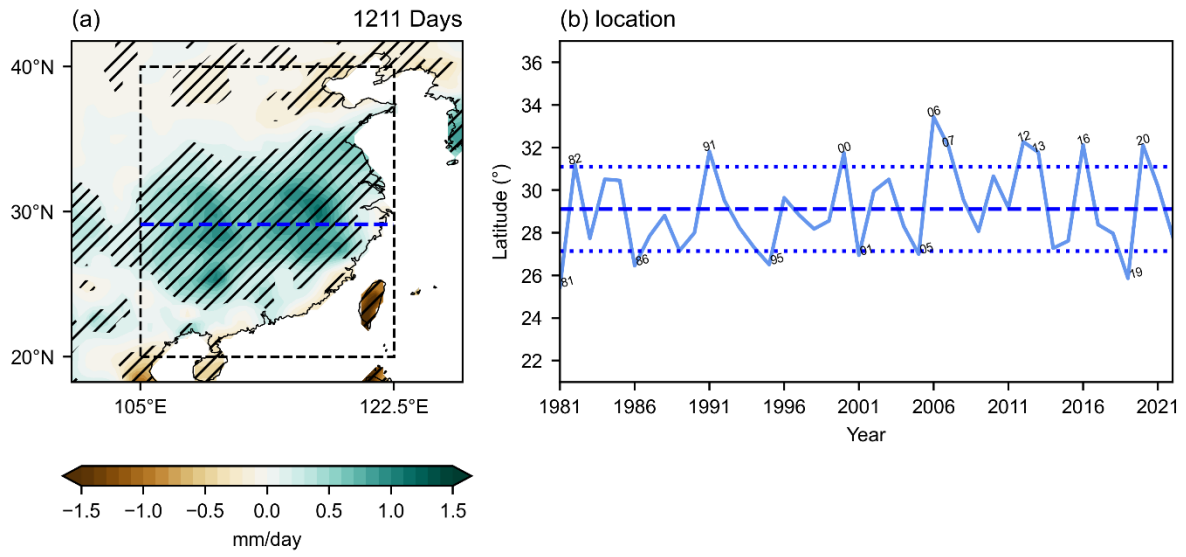


Figure 1. (a) Filtered precipitation anomalies for the Boreal Summer Intraseasonal Oscillation (BSISO) phases 2, 3, and 4 (wet spell). (b) Time series of the BSISO-related precipitation latitudinal location during 1981-2022 for the wet spell.

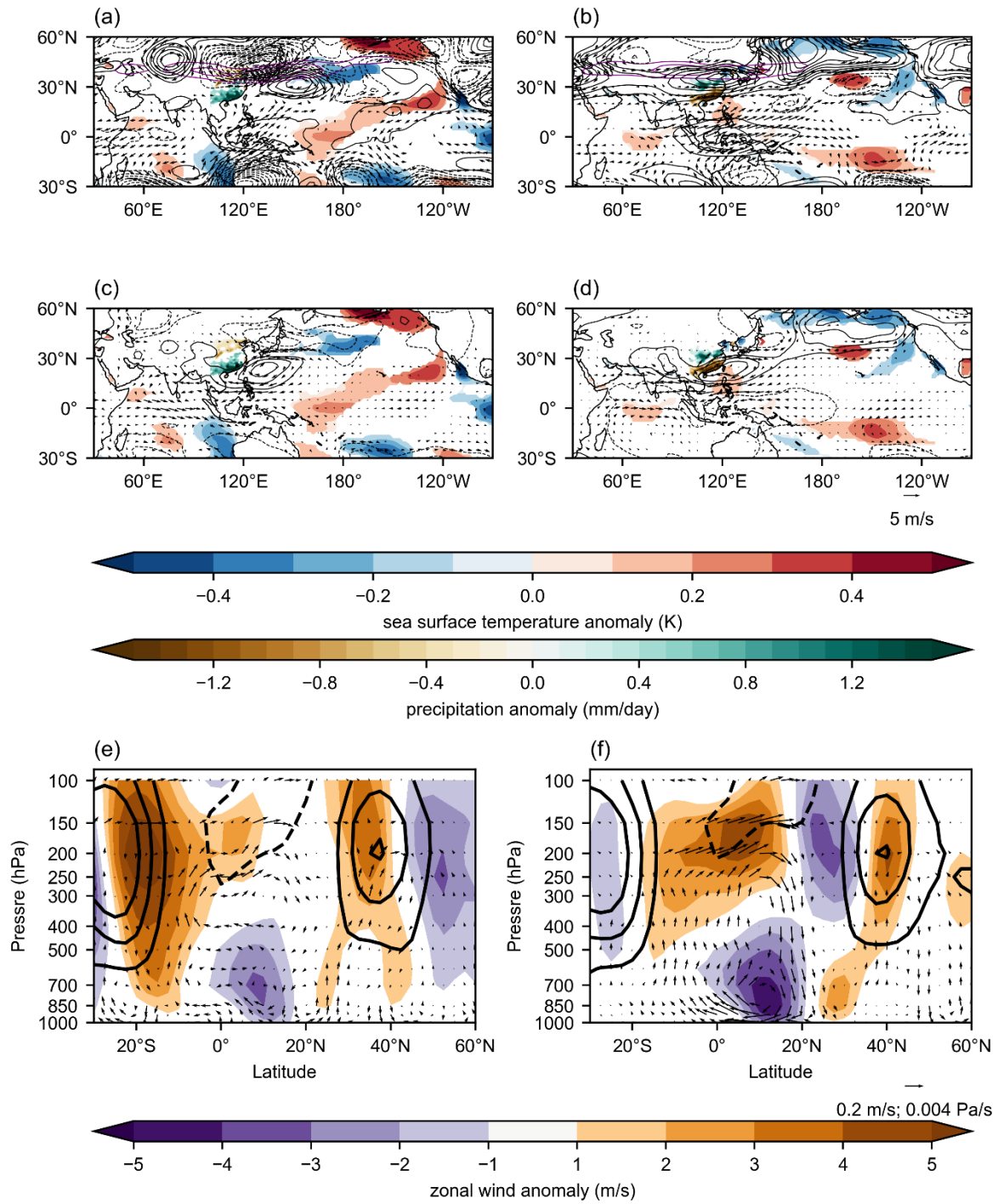


Figure 2. (a-b) Composite horizontal wind anomalies (vectors) and geopotential height anomalies (black contours) at 200hPa (a, b) and 850hPa (c, d) with southward precipitation anomalies (a, c) and northward precipitation anomalies (b, d).

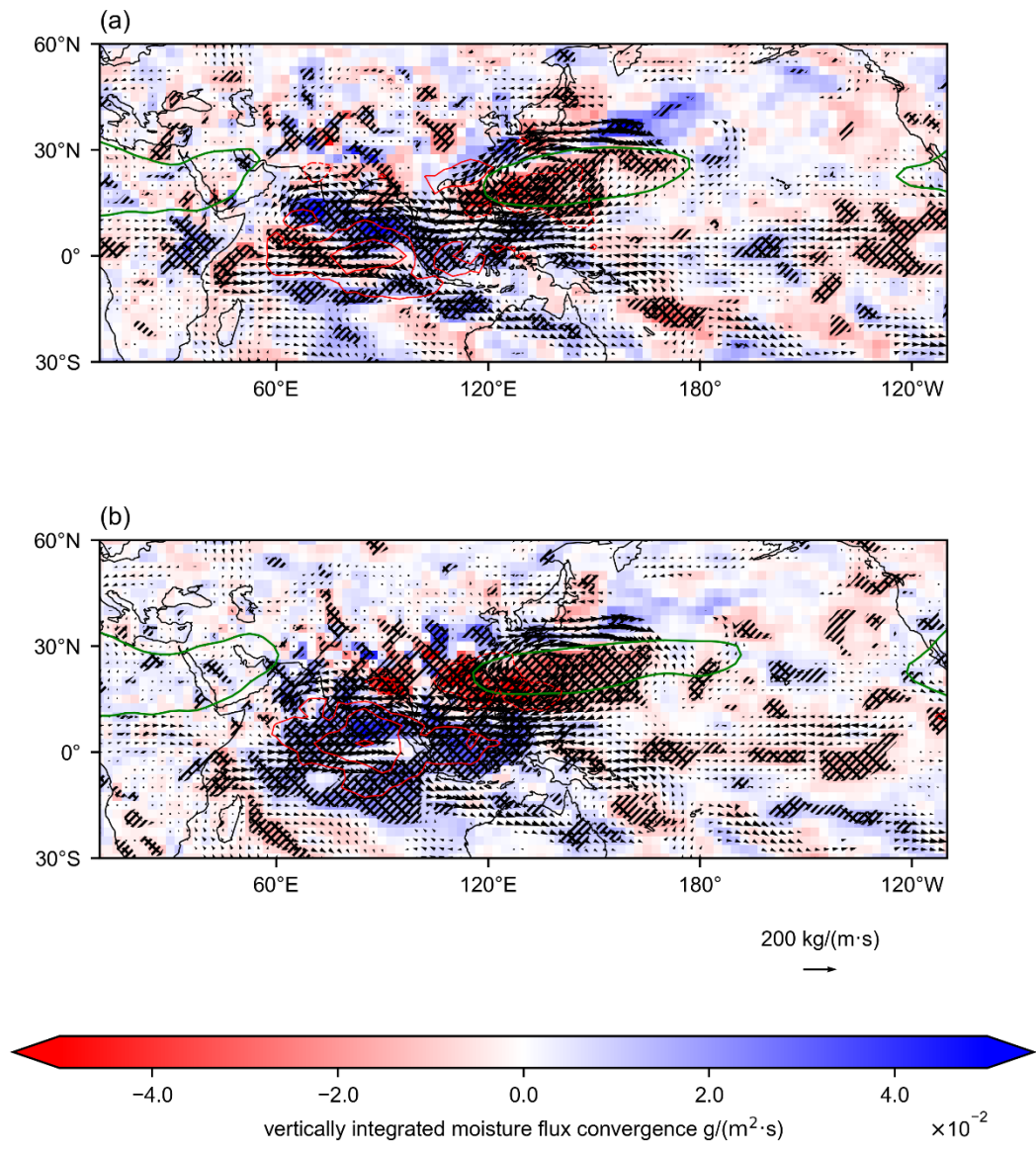


Figure 3. Composite 30-60-day filtered vertically integrated moisture flux (vectors) and its convergence (shading) with (a) southward and (b) northward precipitation anomalies. Green lines represent the subtropical high and red lines represent the 30-60-day filtered outgoing longwave radiation (OLR) anomalies.

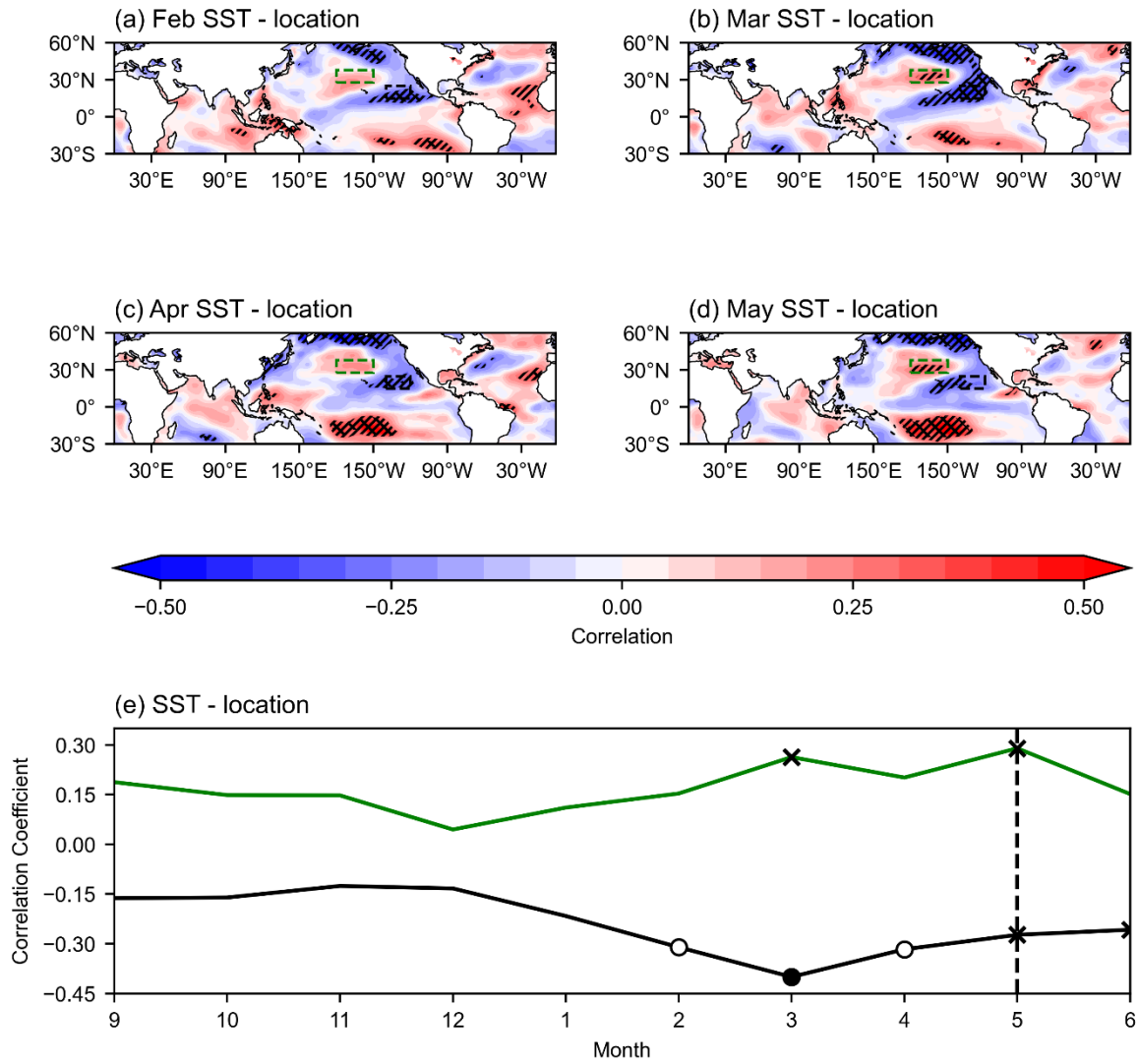


Figure 4. (a-d) The correlation map between SST anomaly in February, March, April, and May and the latitudinal location of BSISO-related precipitation during the wet spell (phases 2, 3, and 4). (e) The lead-lag correlation coefficients between the mean SST in the central northern Pacific (green line) and the northeastern Pacific (black line) from preceding September to June and the latitudinal location of BSISO-related precipitation during the wet spell.